

Title	Ion temperature gradient driven turbulence in the weak density gradient limit
Author(s)	Hamaguchi, Satoshi; Horton, Wendell
Citation	Physics of Fluids B. 2(12) p.3040-p.3046
Issue Date	1990-12
oaire:version	VoR
URL	https://hdl.handle.net/11094/78526
rights	This article may be downloaded for personal use only. Any other use requires prior permission of the author and AIP Publishing. This article appeared in Physics of Fluids B: Plasma Physics 2, 3040 (1990) and may be found at https://doi.org/10.1063/1.859371 .
Note	

Osaka University Knowledge Archive : OUKA

<https://ir.library.osaka-u.ac.jp/>

Osaka University

Ion temperature gradient driven turbulence in the weak density gradient limit

Cite as: Physics of Fluids B: Plasma Physics 2, 3040 (1990); <https://doi.org/10.1063/1.859371>

Submitted: 16 April 1990 . Accepted: 22 August 1990 . Published Online: 01 September 1998

Satoshi Hamaguchi, and Wendell Horton



View Online



Export Citation

ARTICLES YOU MAY BE INTERESTED IN

[Fluctuation spectrum and transport from ion temperature gradient driven modes in sheared magnetic fields](#)

Physics of Fluids B: Plasma Physics 2, 1833 (1990); <https://doi.org/10.1063/1.859455>

[Ion-temperature-gradient-driven transport in a density modification experiment on the Tokamak Fusion Test Reactor](#)

Physics of Fluids B: Plasma Physics 4, 953 (1992); <https://doi.org/10.1063/1.860112>

[Electromagnetic effect on the toroidal ion temperature gradient mode](#)

Physics of Fluids B: Plasma Physics 5, 4030 (1993); <https://doi.org/10.1063/1.860623>



Ion temperature gradient driven turbulence in the weak density gradient limit

Satoshi Hamaguchi^{a)} and Wendell Horton

Institute for Fusion Studies, The University of Texas at Austin, Austin, Texas 78712

(Received 16 April 1990; accepted 22 August 1990)

The anomalous heat transport arising from the ion temperature gradient driven mode or η_i -mode turbulence is extended to the range of the weak density gradient limit ($\eta_i = L_n/L_T \rightarrow \infty$), which is appropriate for H-mode discharges. It is shown that the anomalous ion heat conductivity χ_i with $L_n \rightarrow \infty$ scales as $\chi_i = g(\rho_s/L_T) (cT_i/eB) \exp(-\beta\sigma)$ with $\sigma = (T_e/T_i) (L_T/L_s)$, $\beta \simeq 4$, and $g \simeq 1$. This χ_i scaling is the natural extension for high η_i of the scaling of χ_i for $K = (T_i/T_e) (1 + \eta_i) \lesssim 4$ obtained [Phys. Fluids B 2, 1833 (1990)] from analytical and numerical studies.

I. INTRODUCTION

Anomalous large transport caused by plasma turbulence has recently been a subject of much interest with regard to the confinement properties of various types of magnetic fusion devices. One of the most important problems concerning this subject is to identify the physical mechanism responsible for the anomalous transport and to predict the confinement properties of present and future devices. Recent experimental studies¹⁻⁵ in tokamaks have provided supporting evidence that the ion temperature gradient driven mode or the η_i mode is an important constituent of the turbulence contributing to the anomalous energy loss. Even in the case of the improved energy confinement observed in the so-called H-mode discharges,^{6,7} the ion temperature gradient driven mode could still play an important role for the observed anomalous heat transport.

The ion temperature gradient driven mode (without the presence of the bad magnetic field curvature) is a drift wave microinstability coupled with the ion acoustic waves that is destabilized by the local ion temperature gradient. When the effect of magnetic shear is stronger than the effect of magnetic field curvature, this slab type of ion temperature gradient driven instability is predicted to be excited and to enhance energy transport.^{8,9} This drift-ion acoustic mode is known to be described by a simple fluid model^{8,9} based on the two fluid equations with the polarization drift velocity and adiabatic electrons.

Recently this fluid model of the η_i mode is reinvestigated⁹ analytically and numerically in detail and the scaling of the anomalous ion heat conductivity χ_i is obtained as

$$\chi_i = g(\rho_s/L_n) (cT_i/eB) (\eta_i - \eta_{ic}) \exp(-\alpha s), \quad (1)$$

where $\eta_i = L_n/L_T$ is the ratio of the density gradient scale length to the ion temperature gradient scale length, η_{ic} is its critical value, $s = L_n/L_s$ is the shear parameter, $g \simeq 1$, and $\alpha \simeq 5$. The condition under which Eq. (1) is derived is that η_i is near η_{ic} ($\eta_{ic} < \eta_i \lesssim 3$). It should be noted in Eq. (1) that stronger magnetic shear reduces the anomalous

ion heat conductivity. The same type of shear reduction was observed in early numerical simulations by Horton, Estes, and Biskamp.⁸

In H-mode discharges, it is experimentally observed that the (electron) density profile is flat in a significantly large domain of the bulk plasmas. In such cases, the density gradient scale length L_n is much larger than a typical macroscopic scale length and $\eta_i \rightarrow \infty$. Therefore it is necessary to modify the χ_i scaling given by Eq. (1) in order to calculate the anomalous heat transport in H-mode plasmas. In particular, we need to determine the dependence of α of Eq. (1) on η_i . The goal of the present work is to derive the scaling of the local anomalous heat conductivity χ_i in the flat density profile regime appropriate in explaining the confinement properties in H-mode plasmas.

The conclusion of the present work is summarized in the following χ_i scaling in the weak density gradient limit:

$$\chi_i = g(\rho_s/L_T) (cT_i/eB) \exp(-\beta\sigma) \quad (2)$$

with a numerically obtained parameter $\beta \simeq 4$ and a new shear parameter $\sigma = (T_e/T_i) (L_T/L_s)$. The shear scaling of Eq. (2) is obtained from parametrization of numerical data. More elaborate fitting functions of shear $f(\sigma)$ could be used but the choice of the simple exponential decrease appears sufficient. This is the natural limit of Eq. (1) in the case where $\eta_i \rightarrow \infty$ whereupon $\alpha(\eta_i) \rightarrow \beta(T_e/T_i)/\eta_i$. We note that shear stabilization resulting from parallel compressibility leads to the existence of critical shear σ_{crit} in the weak density gradient limit.

In the next section the fluid model of the η_i mode is reviewed briefly with the use of normalization appropriate for the weak density gradient limit. In Sec. III the linear properties of the η_i mode in the limit of $L_n \rightarrow \infty$ and the critical magnetic shear σ_{crit} are discussed. The scaling of the anomalous ion heat conductivity χ_i obtained from three-dimensional nonlinear numerical simulations is presented in Sec. IV. Section V contains the conclusions.

^{a)}Present address: IBM Thomas J. Watson Research Center, P. O. Box 218, Yorktown Heights, New York 10598.

II. DYNAMICAL EQUATIONS

The nonlinear evolution equations⁹ of the electrostatic ion temperature gradient driven mode are obtained from the two-fluid equations¹⁰ under the assumptions of charge neutrality ($n_i = n_e = n$), constant electron temperature T_e , zero resistivity, and zero electron inertia. The sheared slab configuration of the magnetic field $\mathbf{B} = B[\hat{\mathbf{z}} + (x - x_0)\hat{\mathbf{y}}/L_s]$ is assumed here, which represents a neighborhood of a rational surface given by $x = x_0$. Here L_s denotes the shear scale length, $\hat{\mathbf{x}}$, $\hat{\mathbf{y}}$, and $\hat{\mathbf{z}}$ denote the unit vectors of the usual orthogonal coordinate system (x, y, z) . We split each physical quantity into two parts such as $n = n_0(x) + \tilde{n}$; the unperturbed quantity denoted by subscript 0, which is assumed to be a function of only x , and the perturbed quantity denoted by subscript 1. It is easy to show from the parallel electron momentum balance equation that electrons satisfy a Boltzmann distribution $\tilde{n}/n_0 = e\Phi/T_e$.

The appropriate space-time variables of the ion temperature gradient driven mode are

$$\tilde{x} = \frac{x - x_0}{\rho_s}, \quad \tilde{y} = \frac{y}{\rho_s}, \quad \tilde{z} = \frac{z}{\tau L_T}, \quad \tilde{t} = \frac{tc_s}{\tau L_T},$$

where $\rho_s = c_s/\omega_{ci} = c(m_i T_e)^{1/2}/eB$, $c_s = (T_e/m_i)^{1/2}$ is the sound speed, ω_{ci} is the ion cyclotron frequency, m_i is the ion mass, and $\tau = T_e/T_i$. Assuming that the mean velocity and potential are zero, we obtain the nonlinear evolution equations of the fluctuating quantities,

$$(1 - \nabla_{\perp}^2) \frac{\partial \phi}{\partial \tilde{t}} = -(D + K_T \nabla_{\perp}^2) \frac{\partial \phi}{\partial \tilde{y}} - \nabla_{\parallel} v + \{\phi, \nabla_{\perp}^2 \phi\} - \mu_{\perp} \nabla_{\perp}^4 \phi, \quad (3)$$

$$\frac{\partial v}{\partial \tilde{t}} = -\nabla_{\parallel}(\phi + p) - \{\phi, v\} + \mu_{\parallel} \nabla_{\parallel}^2 v + \mu_{\perp} \nabla_{\perp}^2 v, \quad (4)$$

$$\frac{\partial p}{\partial \tilde{t}} = -K_T \frac{\partial \phi}{\partial \tilde{y}} - \Gamma \nabla_{\parallel} v - \{\phi, p\} + \chi_{\parallel} \nabla_{\parallel}^2 p + \chi_{\perp} \nabla_{\perp}^2 p. \quad (5)$$

Here the nondimensional parameters are given by

$$D = \tau L_T / L_m, \quad K_T = L_T / L_n + 1,$$

$$\Gamma = \gamma / \tau, \quad \sigma = \tau L_T / L_s,$$

and the dependent variable are defined by

$$\phi = \frac{e\tilde{\Phi}}{T_e} \frac{\tau L_T}{\rho_s}, \quad v = \frac{\tilde{v}_{\parallel}}{c_s} \frac{\tau L_T}{\rho_s}, \quad p = \frac{\tilde{p}_i}{p_0} \frac{L_T}{\rho_s},$$

where v_{\parallel} and p_i denote the parallel velocity and the ion pressure, respectively. All the mean quantities used above are evaluated at $x = x_0$. The Poisson bracket and the perpendicular and parallel gradients are given by

$$\{f, g\} = \hat{\mathbf{z}} \cdot \nabla_{\perp} f \times \nabla_{\perp} g = \frac{\partial f}{\partial \tilde{x}} \frac{\partial g}{\partial \tilde{y}} - \frac{\partial f}{\partial \tilde{y}} \frac{\partial g}{\partial \tilde{x}},$$

$$\nabla_{\perp} = \frac{\partial}{\partial \tilde{x}} \hat{\mathbf{x}} + \frac{\partial}{\partial \tilde{y}} \hat{\mathbf{y}},$$

$$\nabla_{\parallel} = \frac{\partial}{\partial \tilde{z}} + \sigma \tilde{x} \frac{\partial}{\partial \tilde{y}}.$$

In deriving Eqs. (3)–(5), we only retain the $\mathbf{E} \times \mathbf{B}$ convective nonlinearity for simplicity.

The domain on which Eqs. (3)–(5) are solved is given by the cubic box $|\tilde{x}| < L_x$, $0 < \tilde{y} < L_y$, and $0 < \tilde{z} < L_z$, L_y and L_z being constants of order unity. The size of the box in the x direction L_x is taken to be large enough, so that when there is magnetic shear ($\sigma \neq 0$), single helicity modes localized at $\tilde{x} = 0$ decay sufficiently as $|\tilde{x}| \rightarrow L_x$. The boundary conditions of Eqs. (3)–(5) are that all the dependent variables vanish at $|\tilde{x}| = L_x$ and are periodic in the \tilde{y} and \tilde{z} directions.

The set of equations (3)–(5) is equivalent to the set of equations used in the earlier work [Eqs. (5)–(7) in Ref. 9]. However, in the present work, where $\eta_i \gg 1$, it is necessary to use a different normalization. For $L_n \gg L_T$ we need to take τL_T to be a typical macroscopic length scale, instead of L_n . Then the time scale must be taken as $\tau L_T / c_s$. The constants $\mu_{\perp, \parallel}$ and $\chi_{\perp, \parallel}$ in Eqs. (3)–(5) are appropriately chosen dissipation rates. The perpendicular diffusion coefficients μ_{\perp} and χ_{\perp} may be taken from the classical collisional transport theory.¹⁰ Using the classical viscosity $\nu_i \sim n T_i / \omega_{ci}^2 \tau_i$ and the classical heat conductivity $\kappa_i \sim T_i / m_i \omega_{ci}^2 \tau_i$, the normalized perpendicular diffusion coefficients μ_{\perp} and χ_{\perp} of Eqs. (3)–(5) are given by

$$\mu_{\perp} = \nu_i \tau L_T / m_i n c_s \rho_s^2 \simeq L_T / c_s \tau_i$$

and

$$\chi_{\perp} = \kappa_i \tau L_T / n c_s \rho_s^2 \simeq L_T / c_s \tau_i,$$

where τ_i denotes the ion collision time. For the high temperature tokamak plasmas of interest the appropriate choice of μ_{\parallel} and χ_{\parallel} is to model the strength of collisionless ion Landau effect in the linear dispersion relation. We use $\mu_{\parallel} = \chi_{\parallel} = 1$ as the approximate collisionless limit for the parallel dissipation rate. We note that these dissipation rates $\mu_{\perp, \parallel}$ and $\chi_{\perp, \parallel}$ are also normalized with the use of macroscopic scale length τL_T , instead of L_n , in contrast to the $\mu_{\perp, \parallel}$ and $\chi_{\perp, \parallel}$ used in Ref. 9.

The cross-field anomalous ion heat conductivity χ_i is given by

$$\chi_i = \frac{\langle \tilde{p}_i \tilde{v}_r \rangle}{-p'_0} = -\frac{\rho_s}{\tau L_T} \left(\frac{c T_e}{e B} \right) \left\langle \frac{\partial \phi}{\partial y} \right\rangle (K_T)^{-1}.$$

Here $\langle \rangle$ denotes a space-time average over fluctuations, which will be defined more precisely later. In the limit of the flat density gradient or $L_n \rightarrow \infty$, we have

$$D \rightarrow 0 \quad \text{and} \quad K_T \rightarrow 1$$

and the fluctuations only become functions of σ and Γ . Since the variation of $\Gamma = \gamma T / T_e$ is limited in most tokamak experiments ($0.5 \lesssim T_i / T_e \lesssim 2$) and the effect of Γ is appreciable only in the case of strong magnetic shear,⁹ we do not develop the dependence of χ_i on Γ here. Therefore, within these limits the anomalous ion heat conductivity χ_i takes the form

$$\chi_i = (\rho_s/L_T) \left(\frac{cT_i}{eB} \right) f(\sigma),$$

where $f(\sigma)$ is a nondimensional function. The goal of this work is to determine the functional form of $f(\sigma)$.

III. LINEAR ANALYSIS

We now consider the linear properties of the system of Eqs. (3)–(5), in the case of the zero density gradient or $D = 0$ and $K_T = 1$. Assuming that the \tilde{y} and \tilde{t} dependence of the linear solutions of this system is given by $\exp \times i(k\tilde{y} - \tilde{\omega}\tilde{t})$, and writing $\phi = \tilde{\phi}(\tilde{x}) \exp i(k\tilde{y} - \tilde{\omega}\tilde{t})$, we obtain the following eigenvalue problem from the linearized equations of Eqs. (3)–(5):

$$\frac{d^2}{d\tilde{x}^2} \tilde{\phi} + \left(-k^2 - \frac{\Omega}{\Omega + 1} + \frac{B + 1}{\Omega + 1} \frac{\sigma^2 \tilde{x}^2}{AB - \sigma^2 \tilde{x}^2 \Gamma} \right) \tilde{\phi} = 0 \quad (6)$$

where

$$A = \Omega + i\mu_{\parallel} k \sigma^2 \tilde{x}^2,$$

$$B = \Omega + i\chi_{\parallel} k \sigma^2 \tilde{x}^2,$$

and $\Omega = \tilde{\omega}/k = \omega/(cT_i/eB)(k_y/L_T)$. Here the perpendicular diffusion coefficients μ_{\perp} and χ_{\perp} are set to be zero for simplicity, $\omega = c\tilde{\omega}/\tau L_T$ is the complex frequency of the mode with physical dimension, and $k = k_y \rho_s$ is the real wave number in the \tilde{y} direction. The \tilde{z} dependence of the solutions is ignored since, in the case of finite shear, the \tilde{z} dependence of the linear solutions only shifts the position of their mode rational surfaces in the x direction. In this section, we only consider an ideal sheared slab or $L_x = \infty$. As discussed in Sec. II, therefore, the boundary condition of Eq. (6) is such that $|\tilde{\phi}(x)| \rightarrow 0$ as $|\tilde{x}| \rightarrow \infty$.

It is easy to show that, if $\mu_{\parallel} = \chi_{\parallel} = \Gamma = 0$, then Eq. (6) gives the following eigenvalue Ω and the eigenfunction $\tilde{\phi}_{l,k}(x)$:

$$\Omega = [1/2(1 + k^2)] \{ [-k^2 - i\sigma(2l + 1)] \pm \sqrt{[k^2 + i\sigma(2l + 1)]^2 - 4i\sigma(2l + 1)(1 + k^2)} \} \quad (7)$$

and

$$\tilde{\phi}_{l,k}(x) = \exp(-\tilde{x}^2/2\Delta_x^2) H_l(\tilde{x}/\Delta_x), \quad (8)$$

where $l(l > 0)$ is the radial mode number associated with the l th eigenvalue of the Weber equation, $\Delta_x^{-2} = i\sigma/\Omega$, and $H_l(z)$ is the l th-order Hermitian function of the complex variable z . The maximum growth rate $\tilde{\gamma}_{\max}$ (measured in $c_s/\tau L_T$) is obtained by varying k and l of Eq. (7) so as to maximize $\tilde{\gamma} = k \text{Im } \Omega$. It should be noted that Ω of Eq. (7) is a function of the combination of shear and radial mode numbers given by $\sigma(2l + 1)$ rather than the shear σ itself. Numerical evaluation of Ω from Eq. (7) shows that for the limit of $\Gamma = \chi_{\perp,\parallel} = \mu_{\perp,\parallel} = 0$ the maximum growth rate is $\tilde{\gamma}_{\max} = 0.20$ with $\sigma(2l + 1) = \tilde{\sigma}_{\max} = 2.4$ and

$k = k_{\max} = 1.3$. If the shear σ is sufficiently small, therefore, the radial mode number l for maximum growth takes a value satisfying $\sigma(2l + 1) = \tilde{\sigma}_{\max}$ and the maximum growth rate $\tilde{\gamma}_{\max}$ is still independent of shear σ . For finite values of Γ , μ_{\parallel} , χ_{\parallel} , μ_{\perp} , and χ_{\perp} , the radial mode number l and the wave number $k = k_y \rho_s$ that give the fastest growing mode take much smaller values than $l_{\max} = (\tilde{\sigma}_{\max}/\sigma - 1)/2$ and k_{\max} calculated from Eq. (7). These parametric dependences of $\tilde{\gamma}(k, l, \sigma)$ are discussed in detail in Ref. 9.

For a fixed radial mode number l , if the magnetic shear σ is small enough such that the condition $k^2 \lesssim |\sigma(2l + 1)| \ll 1$ holds, the eigenvalue Ω of Eq. (7) may be further simplified as

$$\Omega = \frac{1}{2} [-(\sqrt{2\tilde{\sigma}} + k^2) + i(\sqrt{2\tilde{\sigma}} - \tilde{\sigma}) + \mathcal{O}(\tilde{\sigma}^{3/2})], \quad (9)$$

where $\tilde{\sigma} = \sigma(2l + 1)$. We note that $\text{Im } \Omega$ is independent of k up to $\mathcal{O}(\tilde{\sigma})$ in this case.

Following linear perturbation theory,⁹ we now calculate the stabilizing effects of the compressibility of the parallel flow (i.e., $\Gamma \neq 0$) and the parallel diffusion (i.e., μ_{\parallel} , $\chi_{\parallel} \neq 0$). Assuming that $\sigma^2 \Gamma$, $|\mu_{\parallel} k \sigma^2|$, and $|\chi_{\parallel} k \sigma^2|$ are small, we expand the last term of the left-hand side of Eq. (6) as a Taylor series in \tilde{x} . Here we also assume that the mode is localized near $\tilde{x} = 0$, or more precisely, we solve Eq. (6) on a finite domain of \tilde{x} ($|\tilde{x}| \leq L_x$) with the boundary conditions that $|\tilde{\phi}| = 0$ at $|\tilde{x}| = L_x$. Therefore, by taking the values of $\sigma^2 \Gamma$, $|\mu_{\parallel} k \sigma^2|$, and $|\chi_{\parallel} k \sigma^2|$ to be small enough, the Taylor expansion is uniformly convergent. The size of the domain L_x , however, is taken to be large enough, so that the lowest-order solution of Eq. (6) is well approximated by Eq. (8) with the eigenvalue Eq. (7).

Writing Ω as the sum of the lowest-order growth rate Ω_0 given by the right-hand side of Eq. (7) and the remainder Ω_1 , where $|\Omega_1/\Omega_0|$ is also assumed to be small (order of $\sigma^{1/2}$), we expand Eq. (6) in terms of these small parameters. Retaining up to the term of \tilde{x}^4 , we obtain

$$\frac{d^2 \tilde{\phi}}{d\tilde{x}^2} + [E_0 + E_1 - V_0(\tilde{x}) - V_1(\tilde{x})] \tilde{\phi} = 0,$$

where

$$E_0 = -k^2 - \Omega_0/(\Omega_0 + 1),$$

$$E_1 = -\Omega_1/(\Omega_0 + 1)^2,$$

$$V_0 = -\sigma^2 \tilde{x}^2/\Omega_0^2,$$

$$V_1 = [(2\Omega_1/\Omega_0)\sigma^2 \tilde{x}^2 - F\sigma^4 \tilde{x}^4]/\Omega_0^2,$$

and

$$F = \Gamma/\Omega_0^2 - i(\mu_{\parallel} + \chi_{\parallel})k/\Omega_0 + i\chi_{\parallel}k/(\Omega_0 + 1).$$

The lowest-order solution $\tilde{\phi}_0$ of the eigenfunction $\tilde{\phi} = \tilde{\phi}_0 + \tilde{\phi}_1 + \dots$ is given by Eq. (8), which we write as $\tilde{\phi}_{\delta^{(l)}}$, indicating the l th radial eigenmode. The corresponding l th eigenvalue $\Omega_0 = \Omega_0^{(l)}$ is given by Eq. (7). The next-order eigenvalue $\Omega_1 = \Omega_1^{(l)}$ is obtained from the following relation:

$$E_1 = \int_{-\infty}^{\infty} V_1(\tilde{x}) \phi_0^{(l)2} d\tilde{x} \left(\int_{-\infty}^{\infty} \phi_0^{(l)2} d\tilde{x} \right)^{-1}, \quad (10)$$

where the integral is taken over the total domain (i.e., $|\tilde{x}| \leq L_x$ in the case of the finite domain). With the use of $\phi_0^{(l)}$ of Eq. (8), Eq. (10) leads to the following result:

$$\Omega_1^{(l)} = -\sigma^2 F A_l [1/(\Omega_0 + 1)^2 - i\tilde{\sigma}/\Omega_0^2]^{-1}, \quad (11)$$

where $A_l = 3(2l^2 + 2l + 1)/4$. In the case of small $\tilde{\sigma} = \sigma(2l + 1)$, $\Omega_1^{(l)}$ may be simplified with the use of Eq. (9). In this case, $\Omega_0^{(l)2} = -i\tilde{\sigma} + \mathcal{O}(\tilde{\sigma}^{3/2})$ and we have $F = i\Gamma/\tilde{\sigma} + \mathcal{O}(\tilde{\sigma}^{-1/2})$, namely, the effect of parallel diffusion μ_{\parallel} and χ_{\parallel} is smaller than that of the parallel compressibility if $\Gamma \sim \mu_{\parallel} + \chi_{\parallel} \sim \mathcal{O}(1)$. Therefore we obtain

$$\Omega_1^{(l)} = -[3(2l^2 + 2l + 1)/8(2l + 1)^2] i\tilde{\sigma} \Gamma + \mathcal{O}(\tilde{\sigma}^{3/2}).$$

The growth rate $\tilde{\gamma} = \text{Im } \tilde{\omega} = k \text{Im } \Omega^{(l)}$ is then estimated from

$$\begin{aligned} \text{Im } \Omega^{(l)} &= \text{Im } \Omega_0^{(l)} + \text{Im } \Omega_1^{(l)} \\ &= \sqrt{\frac{(2l+1)\sigma}{2}} - \left(\frac{1}{2} + \frac{3(2l^2 + 2l + 1)}{8(2l + 1)^2} \Gamma \right) \\ &\quad \times \sigma(2l + 1) + \mathcal{O}(\tilde{\sigma}^{3/2}). \end{aligned} \quad (12)$$

Formula (12) shows that the parallel compressibility (or nonzero Γ) reduces the growth rate.

We now extrapolate the growth rate given by Eq. (12) to larger magnetic shear and estimate the threshold value of σ . Although Eq. (12) is obtained under the assumption that the second term in the right-hand side is sufficiently smaller than the first term, we estimate the condition for the marginal stability or $\text{Im } \Omega = 0$ by balancing the first term and the second term. The shear parameter σ_{crit} obtained by this balancing is an estimate of the critical magnetic shear and given by

$$\sigma_{\text{crit}} = \frac{2}{(2l+1)} \left(1 + \frac{3(2l^2 + 2l + 1)}{4(2l + 1)^2} \Gamma \right)^{-2},$$

where the l th eigenmode becomes unstable if $\sigma < \sigma_{\text{crit}}$. Thus higher l modes are the first to be stabilized. The most critical shear parameter σ_{crit} is then given by the $l=0$ mode:

$$\sigma_{\text{crit}} = 2(1 + \frac{3}{4}\Gamma)^{-2}. \quad (13)$$

In terms of critical value $(L_s/L_T)_{\text{crit}}$, we have

$$\left(\frac{L_s}{L_T} \right)_{\text{crit}} = \frac{1}{2} \left[1 + \frac{3}{4} \gamma \left(\frac{T_i}{T_e} \right) \right]^2 \left(\frac{T_e}{T_i} \right), \quad (14)$$

where γ is the ratio of the specific heats. If $\Gamma = T_i/T_e = \frac{5}{3}$, we obtain $\sigma_{\text{crit}} \approx 0.40$ and $(L_s/L_T)_{\text{crit}}(T_i/T_e) \approx 2.5$ from Eqs. (13) and (14). For other values of Γ , the critical shear values calculated from Eq. (13) are given by $\sigma_{\text{crit}} = 0.32$ and 0.19 for $\Gamma = 2$ and 3 , respectively. The choice $\Gamma = 3$ may be the appropriate representation of the one-dimensional (1-D) parallel ion dynamics in the collisionless system near the absorption layer $\omega \approx k_{\parallel} v_{\phi}$. For the parameters used for the 3-D numerical simulations pre-

sented in Sec. IV (i.e., $\Gamma = 2$, $\mu_{\parallel} = \chi_{\parallel} = 1.0$, $\mu_{\perp} = \chi_{\perp} = 0.1$, and $k_y \rho_s > 0.2$), the critical magnetic shear becomes $\sigma_{\text{crit}} = 0.54$, which is calculated by means of the initial value code. The critical magnetic shear obtained from the fluid model (with $\Gamma \lesssim 2$) gives a larger value than the formula obtained by Hahm and Tang¹¹ for the gyrokinetic model:

$$(L_s/L_T)_{\text{crit}}^{\text{gyro}} = \frac{3}{2} \sqrt{\pi/2} (1 + T_i/T_e) (2l + 1)$$

or $\sigma_{\text{crit}} = 0.27$ when $T_i = T_e$ and $l=0$. Since the fluid model used in the present work does not necessarily address the physically correct threshold value of magnetic shear, the discrepancy between the fluid model and the gyrokinetic model is expected to exist.

In the next section, we will consider nonlinear saturation of the mode with shear sufficiently smaller than its critical value σ_{crit} . In this case, the linear modes are strongly excited and the fluid model of Eqs. (3)–(5) is considered to give a reasonably accurate description of the mode. The scaling of the anomalous ion heat conductivity χ_i arising from the η_i mode in the flat density profile is presented there and shown to be a decreasing function of the shear σ .

IV. NUMERICAL SIMULATIONS

In this section, results of numerical simulations of the η_i mode in the flat density profile are presented. The initial value code used to solve the nonlinear partial differential equations (3)–(5) is a modification of the code used in Ref. 9, which was modified from the original version of the HIB code.^{12,13} In the initial value code, Fourier representation for the \tilde{y} and \tilde{z} variables and a finite difference scheme for the \tilde{x} variable are employed. At each time step the dependent variables are advanced by means of the predictor–corrector method. The boundary condition is that all the physical variables are periodic in \tilde{y} and \tilde{z} with periods L_y and L_z respectively, and they vanish at $|\tilde{x}| = L_x$, as discussed in Sec. II. We refer to the (m, n) mode of the Fourier representation as the mode whose \tilde{y} and \tilde{z} dependence is given by the phase $2\pi(m\tilde{y}/L_y - n\tilde{z}/L_z)$. The wave numbers \tilde{k}_y and \tilde{k}_z are thus given by $\tilde{k}_y = 2\pi m/L_y$ and $\tilde{k}_z = 2\pi n/L_z$. The rational surface of the (m, n) mode is located at $\tilde{x} = nL_y/m\sigma L_z$ since

$$\nabla_{\parallel} \propto (m\sigma\tilde{x}/L_y - n/L_z) = (m\sigma/L_y) (\tilde{x} - nL_y/m\sigma L_z)$$

for the (m, n) mode. As the initial conditions, small perturbations are given to each (m, n) mode at $\tilde{t} = 0$.

The size of the domain used throughout the following calculations is given by $L_x = 20$, $L_y = 10\pi$, and $L_z = 7.5\pi$, so that the smallest finite wave numbers are $k_y \rho_s = 0.2$ and $k_z \tau L_T = 0.267$ and the distance between the two rational surfaces of the $m=1/n=0$ mode and the $m=1/n=1$ mode in the case of shear $\sigma = 0.1$ is about $13\rho_s$. The equally spaced 150 mesh points are used for discretization of the interval $-L_x < \tilde{x} < L_x$ and 58 modes are chosen for the Fourier representation that cover at least all the unstable modes with $-3 < n < 3$. The diffusion parameters used in the simulations are $\mu_{\parallel} = \chi_{\parallel} = 1.0$ and

$\mu_{\perp} = \chi_{\perp} = 0.1$. As noted in Sec. II, the parallel diffusion parameters $\mu_{\parallel} = \chi_{\parallel} = 1.0$ are chosen so as to model the collisionless ion Landau effect for high temperature plasmas. In order to obtain turbulent saturation, rather than local quasilinear saturation, the background ion pressure gradient is kept constant.⁹

The anomalous ion heat conductivity χ_i is defined by

$$\chi_i = \frac{\langle \tilde{p}_i \tilde{v}_r \rangle}{-p'_{i0}} = -\frac{\rho_s}{L_T} \left(\frac{cT_i}{eB} \right) \left\langle p \frac{\partial \phi}{\partial y} \right\rangle (K)^{-1}. \quad (15)$$

Here the time average $\overline{g(t)}$ of a time-dependent function $g(t)$ is defined by

$$\overline{g(t)} = \lim_{T \rightarrow \infty} \frac{1}{T} \int_0^T g(t) dt$$

and the space average $\langle \rangle$ is defined by

$$\langle \rangle = \frac{1}{\Delta L_y L_z} \int_{-L_x}^{L_x} d\tilde{x} \int_0^{L_y} d\tilde{y} \int_0^{L_z} d\tilde{z}, \quad (16)$$

where Δ denotes the mode width in the \tilde{x} direction. In practice, the time average is taken over a reasonably long time period of T after the saturation is attained. The size of the mode width in the \tilde{x} direction Δ is used as a normalization factor of Eq. (16) so that averaged values calculated from Eqs. (15) do not depend on choice of L_x when the modes are localized. In our simulations, the definition of Δ is given as follows; for a function $f(\tilde{x})$ representing a physical quantity averaged over \tilde{y} and \tilde{z} , we define

$$I(\tilde{x}) = \begin{cases} 1, & \text{if } |f(\tilde{x})| \geq f_{\max}/10, \\ 0, & \text{if } |f(\tilde{x})| < f_{\max}/10, \end{cases}$$

where f_{\max} is the maximum value of $|f(\tilde{x})|$ on $|\tilde{x}| \leq L_x$. Then the mode width Δ is defined by

$$\Delta = \int_{-L_x}^{L_x} I(\tilde{x}) d\tilde{x},$$

which gives a reasonable estimate of the "support" of the localized mode. The fluctuation level of the space-averaged anomalous ion heat conductivity $\chi_i(t) = \langle p_i \tilde{v}_r \rangle / (-p'_{i0})$ is then given by

$$\Delta \chi_i = \{[\chi_i(t) - \chi_i]^2\}^{1/2}. \quad (17)$$

which is shown by error bars in Fig. 1.

The anomalous ion heat conductivity χ_i of Eq. (15) obtained from the 3-D simulations is shown in Fig. 1 as a function of $\sigma/K_T = s/K = (T_e/T_i)/L_s(L_n^{-1} + L_T^{-1})$. The line denoted by $\eta_i = \infty$ in Fig. 1 indicates the shear dependence of χ_i in the case of the flat density profile, where $K_T = 1$ and $s/K = \sigma$. It is shown that magnetic shear reduces the anomalous heat conductivity χ_i approximately as $\chi_i \propto \exp(-\beta\sigma)$ with $\beta \simeq 4$, similar to the χ_i with finite density gradient reported by Hamaguchi and Horton.⁹ In other words, the scaling of the anomalous ion heat conductivity χ_i with the zero density gradient is given by

$$\chi_i = g(\rho_s/L_T) (cT_i/eB) \exp(-\beta\sigma), \quad (18)$$

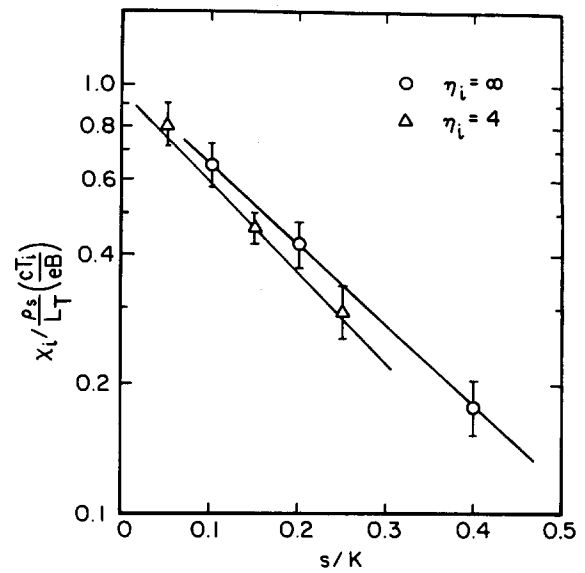


FIG. 1. The anomalous ion heat conductivity χ_i obtained from the 3-D simulations. The parameters used for the simulations are $D=0$, $K_T=1$ for the $\eta_i = \infty$ plot (where $s/K = \sigma$) and $D=0.25$ and $K_T=1.25$ for the $\eta_i = 4$ plot (where $s/K = \sigma/K_T = 0.8\sigma$). The other parameters are $\Gamma = 2$, $\mu_{\parallel} = \chi_{\parallel} = 1.0$, and $\mu_{\perp} = \chi_{\perp} = 0.1$.

where $\beta \simeq 4$, $g \simeq 1$, and $\sigma = (T_e/T_i)(L_T/L_s)$. We note here that this expression of χ_i gives a practically negligibly small value of χ_i at $\sigma = \sigma_{\text{crit}}$.

As a comparison, we also show the $s/K = \sigma/K_T$ dependence of χ_i under the conditions that $D=0.25$ and $K_T=1.25$, or equivalently $\eta_i = 4.0$ and $T_i/T_e = 1$. In this case, χ_i scales as

$$\chi_i = g \frac{\rho_s}{L_T} \left(\frac{cT_i}{eB} \right) \exp\left(-\tilde{\beta} \frac{s}{K}\right) \quad (19)$$

with $\tilde{\beta} \simeq 4.5$, which is slightly larger than $\beta \simeq 4$. In view of the previously obtained χ_i scaling [Eq. (1)] for smaller η_i ($\eta_{ic} < \eta_i \lesssim 3$), this scaling with $\eta_i = 4$ suggests that the parameter $\alpha = \alpha(K)$, which determines strength of shear dependence of χ_i , approximately varies as $\alpha(K) \simeq \tilde{\beta}/K$ when K (or η_i) is sufficiently large. Here $\tilde{\beta} = \tilde{\beta}(K)$ also has a weak dependence on K given by $\tilde{\beta}(K) \simeq 4.5 \rightarrow 4$ as $K \simeq 5 \rightarrow \infty$. Thus taking account of the limit ($\eta_i - \eta_{ic})/L_n \rightarrow 1/L_T$ when $\sigma \ll \sigma_{\text{crit}}$ and $L_n \rightarrow \infty$, we see that there is a smooth connection between the χ_i scaling of Eq. (1) for smaller η_i and the χ_i scaling of Eqs. (18) and (19) for large η_i .

V. CONCLUSIONS

In this work, we extend the previous calculations of the ion temperature gradient driven turbulence to the case of weak density gradients. The new formula of the anomalous ion heat conductivity χ_i resulting from the ion temperature gradient driven turbulence in the limit of zero density gradient is the natural extension of the previously obtained formula⁹ of χ_i . The new formula connects continuously with the previous formula when $L_n \rightarrow \infty$ with a minor adjustment with the numerical coefficient given in Sec. IV. The weak density gradient limit ($L_n \gg L_T$) is important for

the H-mode discharges of tokamak plasmas, where the density profile is known to be flat in the bulk plasma.^{6,7} In the case of improved energy confinement of H mode discharges, microinstabilities such as the η_i mode are considered to be particularly important to account for the observed anomalous heat transport.^{11,14-16}

Considering the region where the magnetic shear effect is stronger than the toroidal curvature effect,¹⁷⁻²² we present the set of equations of the ion temperature gradient driven mode with a dimensionless scaling of both the independent and dependent variables appropriate for the weak density gradient limit. From the scaled set of equations, it is easily shown that the ion temperature gradient driven mode with $L_n = \infty$ depends only on one parameter $\sigma = (T_e/T_i)(L_T/L_s)$ and the anomalous ion heat conductivity χ_i has a form $\chi_i = (\rho_s/L_T)(cT_i/eB)f(\sigma)$, where $f(\sigma)$ is a function of the magnetic shear σ . The present work determines the functional form $f(\sigma)$, as given in Eq. (18).

When magnetic shear is relatively large, the linear analysis for a fixed radial mode number l [Eq. (12)] shows that the linear growth rate decreases with magnetic shear σ , as in the case of the η_i mode with finite L_n .⁹ This is principally due to the parallel compressibility, which leads to the existence of the critical magnetic shear σ_{crit} . An approximate formula for σ_{crit} is given by Eq. (13), which gives $\sigma_{\text{crit}} = 0.40$ for $\Gamma = \frac{5}{3}$ and $\sigma_{\text{crit}} = 0.32$ for $\Gamma = 2$. These numerical values of critical shear σ_{crit} obtained from the fluid model differ some from the σ_{crit} obtained from the gyrokinetic model,¹¹ with the comparison given in Sec. III. When the magnetic shear σ is sufficiently smaller than its critical value σ_{crit} , on the other hand, the modes with high radial mode numbers l are strongly excited and the linear growth rate is shown to be independent of shear.

Three-dimensional nonlinear simulations are used to determine the function of $f(\sigma)$ or shear dependence of χ_i . It is shown that χ_i is a decreasing function of shear, weakly dependent on σ when σ is small and strongly reduced by σ when σ is large. This dependence on shear is parametrized with the exponential fit

$$\chi_i = g(\rho_s/L_T)(cT_i/eB)\exp(-\beta\sigma), \quad (20)$$

where $g \simeq 1$ and $\beta \simeq 4$. Although this exponential dependence of χ_i on σ is one of several possible parametrizations, it expresses with a single parameter β both the weak and strong dependence on σ . The exponential decrease of χ_i with increasing shear provides a sufficiently small value of $\chi_i(\sigma)$ at $\sigma \simeq \sigma_{\text{crit}}$ to be useful without an explicit cutoff at $\sigma = \sigma_{\text{crit}}$. Recent gyrokinetic simulations²³ (with finite η_i) also show a similar tendency in the shear dependence of χ_i for small values of σ ($\sigma \leq 0.05$).

The scaling χ_i of Eq. (20) is the natural extension of the previously obtained χ_i scaling

$$\chi_i = g(\rho_s/L_n)(cT_i/eB)(\eta_i - \eta_{i,c})\exp[-\alpha(K)s], \quad (21)$$

with $s = L_n/L_s$, $K = (T_i/T_e)(1 + \eta_i)$, and $\alpha(K) \simeq 5$ when $(T_i/T_e)(1 + \eta_{i,c}) \leq K \leq 4$. In fact, if $\sigma \ll \sigma_{\text{crit}}$, then $(\eta_i - \eta_{i,c})/L_n \simeq 1/L_T$ and the coefficients of the exponen-

tial functions of Eqs. (20) and (21) become equal. We find that $\alpha(K)$ scales as $\alpha(K) \simeq \beta/K$ when K is large.

Formulas (20) and (21) thus connect smoothly when one takes Eq. (19) or

$$\chi_i = g \frac{\rho_s}{L_T} \left(\frac{cT_i}{eB} \right) \exp \left(-\tilde{\beta} \frac{s}{K} \right), \quad (22)$$

with $\tilde{\beta} = 4-5$ as the χ_i scaling for the large η_i region ($5 \lesssim K < \infty$). Equations (20)–(22) give the scaling of the local anomalous heat conductivity that should explain the anomalous ion heat flux in experiments where the toroidicity is less important than magnetic shear. In H-mode discharges, if the dominant heat transfer is due to the (slab) ion temperature gradient driven turbulence, the anomalous heat conductivity χ_i in the bulk plasma is given by Eqs. (20) and (22), which is of the order of the gyro-reduced Bohm diffusivity [$\simeq (\rho_s/L_T)(cT_i/eB)$]. The improved global energy confinement of H-mode discharges, therefore, would seem to result from an improved local confinement at the edge region where values of η_i are relatively small. Also, we find that the sheared $\mathbf{E} \times \mathbf{B}$ flow $v_E(x)$ in the transition boundary layer reduces the growth rate of the η_i mode for finite values of $L_s v'_E / c_s$.

ACKNOWLEDGMENTS

The authors wish to thank J. P. Mondt and M. N. Rosenbluth for helpful discussions.

This work was supported by U.S. Department of Energy Contract No. DE-FG05-80ET-53088.

¹M. Greenwald, D. Q. Winn, S. Milora, R. Parker, and S. Wolfe, Phys. Rev. Lett. **53**, 352 (1984).

²F. X. Sölder, E. R. Müller, F. Wagner, H. S. Bosch, A. Eberhagen, H. U. Fahrback, G. Fussmann, O. Gehre, K. Gentle, J. Gernhardt, O. Gruber, W. Herrmann, G. Janeschitz, M. Kornherr, K. Krieger, H. M. Mayer, K. McCormick, H. D. Murmann, J. Neuhauser, R. Nolte, W. Poschenreider, H. Röhr, K.-H. Steuer, U. Stroth, N. Tsois, and H. Verbeek, Phys. Rev. Lett. **61**, 1105 (1988).

³R. J. Fonck, R. Howell, K. Jaehnig, L. Roquemore, G. Schilling, S. Scott, M. C. Zarnstorff, C. Bush, R. Goldston, H. Hsuan, D. Johnson, A. Ramsey, J. Schivell, and H. Towner, Phys. Rev. Lett. **63**, 520 (1989).

⁴D. L. Brower, W. A. Peebles, S. K. Kim, N. C. Luhmann, W. M. Tang, and P. E. Phillips, Phys. Rev. Lett. **59**, 48 (1987).

⁵K. Kawahata, K. Adati, R. Akiyama, A. Ando, R. Ando, T. Aoki, D.-G. Bi, J. Fujita, Y. Hamada, S. Hidekuma, S. Hirokura, K. Ida, H. Ikegami, K. Kadota, E. Kako, O. Kaneko, A. Karita, Y. Kawasumi, S. Kitagawa, M. Kojima, T. Koumoto, S. Kubo, Y. Kubota, R. Kumazawa, T. Kuroda, K. Masai, H. Masumoto, A. Mohri, T. Mori, S. Morita, K. Narihara, A. Nishizawa, I. Ogawa, Y. Ogawa, K. Ohkubo, Y. Oka, S. Okajima, S. Okamura, T. Ozaki, A. Sagara, M. Sakamoto, M. Sasao, K. Sato, K. N. Sato, T. Sato, F. Shimbo, S. Tanahashi, Y. Taniguchi, K. Toi, T. Tsuzuki, T. Watari, and H. Yamada, in *Plasma Physics and Controlled Nuclear Fusion Research 1988*, Proceedings of the 11th International Conference, Nice (IAEA, Vienna, 1989), Vol. 1, p. 287.

⁶F. Wagner, G. Becker, K. Behringer, D. Campbell, A. Eberhagen, W. Engelhardt, G. Fussmann, O. Gehre, J. Gernhardt, G. V. Gierke, G. Haas, M. Huang, F. Karger, M. Keilhacker, O. Klüber, M. Kornherr, K. Lackner, G. Lisitano, G. G. Lister, H. M. Mayer, D. Meisel, E. R. Müller, H. Murmann, H. Niedermeyer, W. Poschenreider, H. Rapp, H. Röhr, F. Schneider, G. Siller, E. Speth, A. Stäbler, K. H. Steuer, G. Venus, O. Vollmer, and Z. Yü, Phys. Rev. Lett. **49**, 1408 (1982).

⁷S. M. Kaye, Phys. Fluids **28**, 2327 (1985).

⁸W. Horton, R. D. Estes, and D. Biskamp, Plasma Phys. **22**, 663 (1980).

⁹S. Hamaguchi and W. Horton, Phys. Fluids B **2**, 1833 (1990).

- ¹⁰S. I. Braginskii, in *Review of Plasma Physics*, edited by M. A. Leontovich (Consultants Bureau, New York, 1965), Vol. 1, p. 205.
- ¹¹T. S. Hahm and W. M. Tang, *Phys. Fluids B* **1**, 1185 (1989).
- ¹²W. Park, D. A. Monticello, R. B. White, and A. M. M. Todd, *Bull. Am. Phys. Soc.* **23**, 779 (1978).
- ¹³H. R. Strauss, W. Park, D. A. Monticello, R. B. White, S. C. Jardin, M. S. Chance, A. M. M. Todd, and A. H. Glasser, *Nucl. Fusion* **20**, 628 (1980).
- ¹⁴W. M. Tang, G. Rewoldt, and L. Chen, *Phys. Fluids* **29**, 3715 (1986).
- ¹⁵R. R. Dominguez and R. E. Waltz, *Phys. Fluids* **31**, 3147 (1988).
- ¹⁶D. P. Schissel, R. E. Stockdale, H. St. John, and W. M. Tang, *Phys. Fluids* **31**, 3738 (1988).
- ¹⁷W. Horton, D.-I. Choi, and W. M. Tang, *Phys. Fluids* **24**, 1077 (1981).
- ¹⁸P. N. Guzdar, L. Chen, W. M. Tang, and P. H. Rutherford, *Phys. Fluids* **26**, 673 (1983).
- ¹⁹A. Jarmén, P. Andersson, and J. Weiland, *Nucl. Fusion* **27**, 941 (1987).
- ²⁰R. E. Waltz, *Phys. Fluids* **31**, 1962 (1988).
- ²¹H. Nordman and J. Weiland, *Nucl. Fusion* **29**, 251 (1989).
- ²²F. Romanelli, *Phys. Fluids B* **1**, 1018 (1989).
- ²³R. D. Sydora, T. S. Hahm, W. W. Lee, and J. M. Dawson, *Phys. Rev. Lett.* **64**, 2015 (1990).